Stellar Production Rates of Carbon and Its Abundance in the Universe

H. Oberhummer, *et al.*

Science **289**, 88 (2000);
DOI: 10.1126/science.289.5476.88

Science (print ISSN 0036-8075; online ISSN 1095-9203) is published weekly, except the last week in December, by the American Association for the Advancement of Science, 1200 New York Avenue NW, Washington, DC 20005.

suggests that the *fw2.2* phenotype is probably not caused by differences within the coding region of *ORFX*, but by one or more changes upstream in the promoter region of *ORFX*. Variation in upstream regulatory regions of the *teosinte branched1* gene has also been implicated in the domestication of maize (*21*). However, differences in fruit size imparted by the different *fw2.2* alleles may be modulated by a combination of sequence changes in the coding and upstream regions of *ORFX* (*22*).

A reduction in cell division in carpels of the small-fruited NIL is correlated with overall higher levels of ORFX transcript, suggesting that ORFX may be a negative regulator of cell division. Whether the ORFX and RAX proteins share common properties other than predicted three-dimensional structure and control of cell division awaits future experimentation. An affirmative result may reflect an ancient and common origin in the processes of cell cycle regulation in plants and animals.

References and Notes

1. J. Doebley, A. Stec, J. Wendel, M. Edwards, *Proc. Natl. Acad. Sci. U.S.A.* **87**, 9888 (1990).
2. J. Smartt and N. W. Simmonds, *Evolution of Crop Plants* (Longman, London, 1995).
3. C. M. Rick, R. W. Zobel, J. F. Fobes, *Proc. Natl. Acad. Sci. U.S.A.* **71**, 835 (1974).
4. A. H. Paterson *et al.*, *Genetics* **127**, 181 (1991).
5. S. D. Tanksley, *Annu. Rev. Genet.* **27**, 205 (1993).
6. S. Grandillo, H. M. Ku, S. D. Tanksley, *Theor. Appl. Genet.* **99**, 978 (1999).
7. K. B. Alpert, S. Grandillo, S. D. Tanksley, *Theor. Appl. Genet.* **91**, 994 (1995).
8. K. B. Alpert and S. D. Tanksley, *Proc. Natl. Acad. Sci. U.S.A.* **93**, 15503 (1996).
9. Details are available at *Science* Online at www.sciencemag.org/feature/data/1050401.shl.
10. The Expand Long Template PCR System (Boehringer Mannheim) was used.
11. Constructs were electroporated into *Agrobacterium tumefaciens* strain ABI-A208 (Monsanto, St. Louis, MO).
12. A. Frary and E. D. Earle, *Plant Cell Rep.* **16**, 235 (1996).
13. The presence of the transgene was assayed by PCR and Southern hybridization analyses.
14. A total of 11 primary transformants were generated for cos50. Although all of these plants carried *nptII*, only two individuals (fw71 and fw107) contained the *L. pennellii* portion of the transferred DNA, as determined by PCR analysis with primers designed from the *L. pennellii* sequence of cos50.
15. Cosmid sequencing is described at *Science* Online at www.sciencemag.org/feature/data/1050401.shl.
16. RT-PCR is described at *Science* Online at www.sciencemag.org/feature/data/1050401.shl.
17. 5′ and 3′ rapid amplification of cDNA ends (RACE) is described at *Science* Online at www.sciencemag.org/feature/data/1050401.shl.
18. The predicted ORFX protein was compared to a training set of 594 structures (chosen from the Protein Data Base to eliminate redundancy) by using the LOOPP algorithm (J. Meller and R. Elber, in preparation). See also www.tc.cornell.edu/reports/NIH/resource/CompBiologyTools/loopp/.
19. The three-dimensional structure of c-H-ras p21 (6q21) is shown at *Science* Online at www.sciencemag.org/feature/data/1050401.shl.
20. Reviewed in S. R. Sprang, *Curr. Opin. Struct. Biol.* **7**, 849 (1997).
21. R Wang, A. Stec, J. Hey, L. Lukens, J. Doebley, *Nature* **398**, 236 (1999).
22. P. C. Phillips, *Trends Genet.* **15**, 6 (1999).

23. Seed number is included in the analysis because reduced fertility, as evidenced by reduced seed per fruit, can decrease fruit size. Thus, these data show that the change in fruit size associated with cos50 is not a byproduct of reduced fertility.
24. The alignment of LpORFX and LeORFX with a total of 26 genes is shown at *Science* Online at www.sciencemag.org/feature/data/1050401.shl.

25. We thank J. Nasrallah, C. Aquadro, J. Doebley, K. Schmid, and W. Swanson for critical review of the manuscript. We also thank C. Lewis and N. van Eck for technical assistance. Supported by grants to S.D.T. from the National Research Initiative Cooperative Grants Program, U.S. Department of Agriculture Plant Genome Program (No. 97-35300-4384); the National Science Foundation (No. DBI-9872617); and the Binational Agricultural Research and Development Fund (No. US 2427-94) and by a grant from the NIH NCRR (National Center for Research Resources) to R.E. for development of LOOPP at Cornell Theory Center. We dedicate this paper to the memory of Dr. Kevin Alpert whose research inspired this work.

14 March 2000; accepted 4 May 2000

Stellar Production Rates of Carbon and Its Abundance in the Universe

H. Oberhummer,[1]* A. Csótó,[2] H. Schlattl[3]

The bulk of the carbon in our universe is produced in the triple-alpha process in helium-burning red giant stars. We calculated the change of the triple-alpha reaction rate in a microscopic 12-nucleon model of the ^{12}C nucleus and looked for the effects of minimal variations of the strengths of the underlying interactions. Stellar model calculations were performed with the alternative reaction rates. Here, we show that outside a narrow window of 0.5 and 4% of the values of the strong and Coulomb forces, respectively, the stellar production of carbon or oxygen is reduced by factors of 30 to 1000.

The formation of ^{12}C through the triple-alpha process takes place in two sequential steps in the He-burning phase of red giants. In the first step, the unstable ^{8}Be with a lifetime of only about 10^{-16} s is formed in a reaction equilibrium with the two alpha particles, $\alpha + \alpha \rightleftharpoons {}^{8}\mathrm{Be}$. In the second step, an additional alpha particle is captured, $^{8}\mathrm{Be}(\alpha,\gamma)^{12}\mathrm{C}$. Without a suitable resonance in ^{12}C, the triple-alpha rate would be much too small to account for the ^{12}C abundance in our universe. Hoyle (*1*) suggested that a resonance level in ^{12}C, at about 300 to 400 keV above the three-alpha threshold, would enhance the triple-alpha reaction rate and would explain the abundance of ^{12}C in our universe. Such a level was subsequently found experimentally when a resonance that possessed the required properties was discovered (*2*, *3*). It is the second 0^+ state in ^{12}C, denoted by 0_2^+. Its modern parameters (*4*) are $\varepsilon = (379.47 \pm 0.18)$ keV, $\Gamma = (8.3 \pm 1)$ eV, and $\Gamma_\gamma = (3.7 \pm 0.5)$ meV, where ε is the resonance energy in the center-of-mass frame relative to the three-alpha threshold, and Γ and Γ_γ are the total width and radiative width, respectively.

The isotope ^{12}C is synthesized further in the He burning in red giants by alpha capture to the O isotope ^{16}O, leading to an abundance ratio in the universe of $^{12}\mathrm{C}:^{16}\mathrm{O} \approx 1:2$ (*5*). If the carbon abundance in the universe were suppressed by orders of magnitude, no carbon-based life could have developed in the universe. But the production of O is also necessary because no spontaneous development of carbon-based life is possible without the existence of water.

Here, we investigated the abundance ratios of C and O by starting from slight variations of the strength of the nucleon-nucleon (N-N) interaction with a microscopic 12-nucleon model. In previous studies, only hypothetical ad hoc shifts of the resonance energy of the 0_2^+ state were considered (*6*). Some preliminary results of our calculations are reported elsewhere (*7*).

The resonant reaction rate for the triple-alpha process ($r_{3\alpha}$) proceeding via the ground state of ^{8}Be and the 0_2^+ resonance in ^{12}C is given approximately by (*5*)

[1]Institute of Nuclear Physics, Vienna University of Technology, Wiedner Hauptstrasse 8-10, A-1040 Vienna, Austria. [2]Department of Atomic Physics, Eötvös University, Pázmány Péter Sétány 1/A, H-1117 Budapest, Hungary. [3]Max-Planck-Institut für Astrophysik, Karl-Schwarzschild-Str. 1, D-85741 Garching, Germany.

*To whom correspondence should be addressed. E-mail: ohu@kph.tuwien.ac.at

$$r_{3\alpha} = 3^{3/2} N_\alpha^3 \left(\frac{2\pi\hbar^2}{M_\alpha k_B T}\right)^3 \frac{\Gamma_\gamma}{\hbar} \exp\left(-\frac{\varepsilon}{k_B T}\right) \quad (1)$$

where M_α and N_α are the mass and the number density of the alpha particle, and $\hbar$ and k_B are Planck's and Boltzmann's constant, respectively. The temperature of the stellar plasma is given by T.

The two quantities in Eq. 1 that change their value by varying the strength of the N-N interaction are ε and Γ_γ of the 0_2^+ resonance in ^{12}C. These quantities are calculated in a microscopic 12-body, three-alpha cluster model of ^{12}C. The cluster model assumes relatively simple harmonic-oscillator shell-model states for the alpha particles and describes with high precision the relative motions between the clusters, which are the most important degrees of freedom (*8*). The model treats ^{12}C as a system of 12 interacting nucleons, properly takes into account the Pauli principle, and is free of any nonphysical center-of-mass excitation. The only input parameter in the model is the effective N-N interaction. To explore and understand any dependence of the results on the chosen interaction, we used several different sets of forces, including the Minnesota (MN) and modified Hasegawa-Nagagta (MHN) interactions (*9*–*12*). These interactions give a good overall description of the $\alpha + \alpha$ scattering and the ^{12}C levels (*8*).

As a first step of our calculations, we fine-tuned each force (by slightly changing their exchange-mixture parameters) to fix ε in Eq. 1 at its experimental value. Then we performed calculations for ε and Γ_γ while slightly varying the strengths of the N-N forces. For a given set of forces, all repulsive and attractive terms of the interaction are multiplied by a factor p, which was set between 0.994 and 1.006. Thus, the calculations with $p = 1.0$ correspond to the physical strength of the N-N interaction and reproduce the experimental value of ε.

We find that the value of Γ_γ is minimally changed by the small variations of the N-N interactions, leading to negligible changes in $r_{3\alpha}$. Thus, in the stellar model calculations we can fix Γ_γ to its experimental value in all cases. The resonance energy ε, however, is rather sensitive to variations in the N-N force, leading to large changes in the triple-alpha rate $r_{3\alpha}$.

In addition to the strong interaction, the triple-alpha reaction rate depends on another fundamental force, the electromagnetic interaction. The strength of the Coulomb interaction between the protons is proportional to the fine structure constant α_f. To see the sensitivity of $r_{3\alpha}$ to changes in α_f, we performed calculations for the energy of the 0_2^+ resonance of ^{12}C while slightly varying α_f from its experimental value (1/137.036), much the same way as with the strong N-N interaction. We found that varying α_f leads to a smaller and reversed effect for the change in the energy of the 0_2^+ resonance. This result is logical because the Coulomb interaction between the alpha clusters has a different sign and is weaker than the strong interaction.

The ^{16}O$(\alpha,\gamma)^{20}$Ne reaction is nonresonant, so variations in the strengths of the strong or Coulomb forces can have only small effects on its reaction rate. The ^{12}C$(\alpha,\gamma)^{16}$O process may look more dangerous because its cross section is strongly affected by subthreshold states in the ^{16}O nucleus (*5*). However, if the N-N force is made weaker, then the subthreshold states become less bound, thereby enhancing the ^{12}C$(\alpha,\gamma)^{16}$O cross section. Therefore, in the case of a weaker force, the small C/O ratio is still decreased. An analogous reasoning holds for a stronger force. Thus, without doing any calculation for the ^{12}C$(\alpha,\gamma)^{16}$O and ^{16}O$(\alpha,\gamma)^{20}$Ne reactions with the modified forces, we can conclude that their effect would strengthen our hypothesis regarding carbon and oxygen production.

For stars with masses more than ~0.9 solar mass ($M_\odot$), the temperatures in the center can reach the burning temperature of He, thus producing C by the triple-alpha process (*13*). Depending on the exact conditions in the center, some C may be further fused to O by capturing an additional alpha particle. When all He in the center of the star is consumed, the triple-alpha reaction proceeds in shells around this core. In this phase, two burning shells are present, one shell that burns H and one that burns He, and are separated by a region of radiative energy transport.

In stars with masses $\lesssim 8M_\odot$, this double shell-burning structure is thermally unstable (*14*), creating thermal pulses with high rates of mass loss. In this phase these stars lose the whole envelope, i.e., the layers above the H-burning shell, creating planetary nebulae (PNe) with a white dwarf in the center. During one thermal pulse, the H- and He-burning shells alternately provide the energy source of the star. When the energy-release of the He shell approaches its maximum, a convective zone develops. The C and O produced by fusion of He is dredged into layers that might, in a latter part of the pulse, be covered by the convective envelope (*15*). In this way, they are transported to the surface where they are blown away by the stellar wind, creating a heavy-element enriched PNe.

Unfortunately, the exact amount of C and O dredged up is uncertain, because it depends on poorly understood processes at the boundary of the convective layers, such as overshooting or rotational mixing (*16*). Thus, theoretical predictions about the composition of PNe are not accurate. But here we were only interested in the change of C and O abundances under modifications of the 0_2^+ resonance energy in ^{12}C. Because we did not expect that additional mixing processes at the formal boundaries of convective zones are altered by changes in nuclear physics, we believed the relative changes of the C and O abundances would remain independent of such mixing processes.

In massive stars ($M > 8M_\odot$), advanced burning phases take place until the center reaches nuclear matter densities, where the collapsing matter bounces back and explodes in supernovae (SNe). Although further nuclear reactions take place in the explosion, the relative abundances of C and O are not believed to change drastically.

The composition of the interstellar material (ISM) is a mixture of ejecta from stars with different masses. To determine which stellar mass contributes to the total amount of C and O in the ISM, one has to know these abundances in the PNe or SNe and the mass function, which provides the number of stars with a certain mass. At present, it is unclear which stars most enrich the ISM with C and O. Various calculations of stellar yields of massive stars exist (*17*–*19*), which agree that O seems to be dominantly produced in these stars, whereas the C situation is less clear. Recent investigations appear to support the assessment that stars with masses of $1 - 8M_\odot$ are the major producers of C (*20*, *21*).

The calculations with the reaction rates from the slightly modified strong or Coulomb inter-

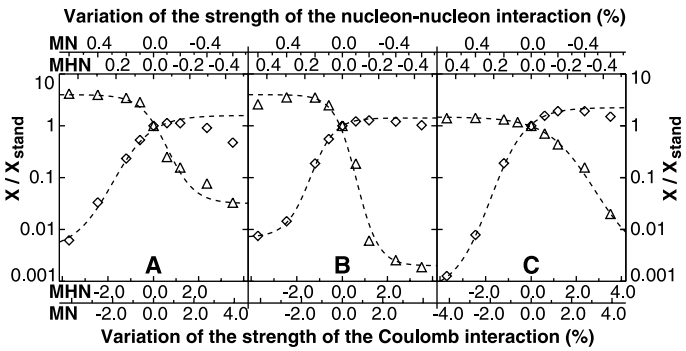

Fig. 1. The change of the C and O mass abundances through variations of the strengths of the strong and Coulomb interactions. The C mass abundance, X_C (△), and the O mass abundance, X_O (◇), are shown in (**A**), (**B**), and (**C**) for stars with masses 20, 5, and $1.3M_\odot$, respectively, in units of the standard values, X_{stand}. The variations of the strength of the strong and Coulomb interaction are given in the upper and lower scales for the two effective N-N forces MHN and MN. Dashed curves are drawn to show the trends.

action were performed with a contemporary stellar evolution code, which contains the most recent physics input (*22*). In particular, use of this code can produce up-to-date solar models (*23*) and can allow one to follow the evolution of low-mass stars through the thermal pulses of asymptotic giant branch (AGB) stars (*24*). The nuclear network is designed preferentially to calculate the H- and He-burning phases in low-mass stars. Additionally, the basic reactions of C- and O-burning are included, which may destroy the produced C and O in massive and intermediate-mass stars.

We performed stellar model calculations for a typical massive, intermediate-mass, and low-mass star with masses 20, 5, and $1.3M_{\odot}$, respectively. The stars are followed from the onset of H-burning until the third thermal pulse in the AGB, or until the core temperature reaches 10^9 K in the case of the $20M_{\odot}$ star (the nuclear network is not sufficient to go beyond this phase). For the $1.3M_{\odot}$ star, which loses its envelope by stellar winds during the thermal-pulse phase, the maximum C and O abundances in the He-burning region have been extracted. By taking the maximum abundances in this region, we have a measure of how much the envelope of the star can be enriched by C or O, irrespective of how efficient the dredge-up of heavy elements is compared with our model.

For the three stellar masses, the evolution is calculated with different values of the resonance energy in the triple-alpha reaction within a range to cover variations in the strength of the strong and Coulomb interaction up to 0.5 and 4%, respectively. The resulting modifications in the C and O abundances are shown (Fig. 1) with respect to the case, where the standard value of the resonance energy has been used (i.e., with no variations of the strength of the strong or Coulomb interaction). Because each shift in the resonance energy can be identified with a variation in the strength of the N-N or Coulomb interaction, we scaled the upper and lower ordinate with variations in these quantities. Our calculations indicate that the behavior of the residual alpha-alpha interaction, and thus that of the resonance energy of the 0_2^+ state, is expected to lie somewhere between the predictions of two of our effective N-N interactions, the MN (*10*, *11*) and the MHN (*12*) forces. Therefore, we show the abundances calculated only with these two effective N-N interactions (Fig. 1).

A saturation of the C production is reached with increasing N-N interaction (very pronounced for the $5M_{\odot}$ star) because no alpha particles are available below the He-burning front. Thus, the star does not gain additional energy from the $^{12}C(\alpha,\gamma)^{16}O$ reaction. The stellar core contracts more rapidly and C-destroying $^{12}C + {}^{12}C$ reactions ignite earlier. For O, a similar behavior can be observed with decreasing N-N interaction strength. Because the temperatures where the triple-alpha reactions set in are enhanced with decreasing N-N force, the temperatures below the He-burning shell are much higher than in the standard case, and $^{16}O + \alpha$ reactions can destroy the previously generated O more efficiently than in the standard case (0%).

We conclude that a change of more than 0.5% in the strength of the strong interaction or more than 4% change in the strength of the Coulomb force would destroy either nearly all C or all O in every star. This implies that irrespective of stellar evolution the contribution of each star to the abundance of C or O in the ISM would be negligible. Therefore, for the above cases the creation of carbon-based life in our universe would be strongly disfavored. The anthropically allowed strengths of the strong and electromagnetic forces also constrain the Higgs vacuum expectation value (*25*) and yield tighter constraint on the quark masses than do the constraints from light nuclei (*26*). Therefore, the results of this work are relevant not only for the anthropic cosmological principle (*27*), but also for the mathematical design of fundamental elementary particle theories.

References and Notes

1. D. N. F. Dunbar, R. E. Pixley, W. A. Wenzel, W. Whaling, *Phys. Rev.* **92**, 649 (1953).
2. F. Hoyle, D. N. F. Dunbar, W. A. Wenzel, *Phys. Rev.* **92**, 1095 (1953).
3. C. W. Cook, W. A. Fowler, T. Lauritsen, *Phys. Rev.* **107**, 508 (1957).
4. V. S. Shirley, Ed., *Table of Isotopes, Volume I* (Wiley, New York, ed. 8, 1996).
5. C. E. Rolfs and W. S. Rodney, *Cauldrons in the Cosmos* (Univ. of Chicago Press, Chicago, 1988).
6. M. Livio, D. Hollowell, A. Weiss, J. W. Truran, *Nature* **340**, 281 (1989).
7. H. Oberhummer, A. Csótó, H. Schlattl. Print available at http://xxx.lanl.gov/abs/astro-ph/9908247.
8. R. Pichler, H. Oberhummer, A. Csótó, S. A. Moszkowski, *Nucl. Phys. A* **618**, 55 (1997).
9. A. B. Volkov, *Nucl. Phys.* **74**, 33 (1965).
10. I. Reichstein and Y. C. Tang, *Nucl. Phys. A* **158**, 529 (1970).
11. D. R. Thompson, M. LeMere, Y. C. Tang, *Nucl. Phys. A* **286**, 53 (1977).
12. H. Furutani *et al.*, *Prog. Theor. Phys. Suppl.* **68**, 193 (1980).
13. R. Kippenhahn and A. Weigert, *Stellar Structure and Evolution* (Springer-Verlag, Berlin, 1990).
14. M. Schwarzschild and A. R. Härm, *Astrophys. J.* **142**, 855 (1965).
15. I. Iben and A. Renzini, *Ann. Rev. Astron. Astrophys.* **21**, 271 (1983).
16. A. Weiss, P. A. Denissenkov, C. Charbonnel, *Astron. Astrophys.* **356**, 181 (2000).
17. S. E. Woosley and T. A. Weaver, *Astrophys. J. Suppl. Ser.* **101**, 181 (1995).
18. K. Nomoto *et al.*, *Nucl. Phys. A* **616**, 79 (1997).
19. A. Maeder, *Astron. Astrophys.* **264**, 105 (1992).
20. F. X. Timmes, S. E. Woosley, T. A. Weaver, *Astrophys. J. Suppl. Ser.* **98**, 617 (1995).
21. R. B. C. Henry, K. B. Kwitter, J. A. Bates, *Astrophys. J.*, in press (e-print available at http://xxx.lanl.gov/abs/astro-ph/9910347).
22. A. Weiss and H. Schlattl, *Astron. Astrophys. Suppl.*, **144**, 487 (2000) (e-print available at http://xxx.lanl.gov/abs/astro-ph/9912310).
23. H. Schlattl and A. Weiss, *Astron. Astrophys.* **347**, 272 (1999).
24. J. Wagenhuber and A. Weiss, *Astron. Astrophys.* **286**, 121 (1994).
25. E. T. Jeltema and M. Sher, *Phys. Rev. D* **61**, 017301 (2000).
26. C. J. Hogan, e-print available at http://xxx.lanl.gov/abs/astro-ph/9909295.
27. J. D. Barrow and F. J. Tipler, *The Anthropic Cosmological Principle* (Oxford Univ. Press, Oxford, 1986).

28. Supported in part by the Fonds zur Wissenschaftlichen Forschung in Österreich (P10361-PHY), the OTKA Fund (D32513), the Education Ministry (FKFP-0242/2000), the Academy (BO/00520/98) in Hungary, and by the John Templeton Foundation (938-COS153).

14 March 2000; accepted 17 May 2000

Topographic Mapping of the Quantum Hall Liquid Using a Few-Electron Bubble

G. Finkelstein,[1] P. I. Glicofridis,[1] R. C. Ashoori,[1] M. Shayegan[2]

A scanning probe technique was used to obtain a high-resolution map of the random electrostatic potential inside the quantum Hall liquid. A sharp metal tip, scanned above a semiconductor surface, sensed charges in an embedded two-dimensional (2D) electron gas. Under quantum Hall effect conditions, applying a positive voltage to the tip locally enhanced the 2D electron density and created a "bubble" of electrons in an otherwise unoccupied Landau level. As the tip scanned along the sample surface, the bubble followed underneath. The tip sensed the motions of single electrons entering or leaving the bubble in response to changes in the local 2D electrostatic potential.

Since the discovery of the integer quantum Hall effect (QHE) in a two-dimensional electron gas (2DEG), electron localization has been proposed to play a key role in the phenomenon (*1*). In GaAs heterostructures, the random potential responsible for localization derives mainly from randomly situated ionized donors, located between the submerged 2DEG and the sample surface. Although this picture remains widely used, it has proven difficult to quantify the random potential experimentally. Conductivity measurements, the